Supplemental Information
Molecular Cell, *Volume 39*

STAT3 Activation of miR-21 and miR-181b-1 via PTEN and CYLD Are Part of the Epigenetic Switch Linking Inflammation to Cancer

Dimitrios Iliopoulos, Savina A. Jaeger, Heather A. Hirsch, Martha L. Bulyk, and Kevin Struhl

Supplemental Experimental Procedures

Lever Algorithm Analysis

We utilized the MultiZ 17-way alignment of: mouse (Feb 2006, mm8); rat (Nov 2004, rn4); rabbit (May 2005, oryCun1); human (Mar. 2006, hg18); chimp (Mar. 2006, panTro2); macaque (Jan 2006, rheMac2); dog (May 2005, canFam2); cow (Mar 2005, bosTau2); armadillo (May 2005, dasNov1); elephant (May 2005, loxAfr1); tenrec (Jul 2005, echTel1); opossum (Jan 2006, monDom4); chicken (Feb 2004, galGal2); frog (Aug 2005, xenTro2); zebrafish (Mar 2006, danRer4); Tetraodon (Feb 2004, tetNig1); Fugu (Aug 2002, fr1).

The MultiZ alignment was performed by Genome Bioinformatics Group of UC Santa Cruz. The mouse (mm8) sequence and annotation data were downloaded from the Genome Browser FTP server (ftp://hgdownload.cse.ucsc.edu/goldenPath/mm8/). Repeats from RepeatMasker and Tandem Repeats Finder (with period of 12 or less) were masked out (RepeatMasker January 12 2005 version with RepBase libraries: RepBase Update 9.11, RM database version 20050112). The exon coding regions were also masked out by utilizing the annotation database. For each RefSeq mouse gene and the corresponding 11 alignments, we considered in our Lever analysis the sequence regions from 10 (2) kb upstream through to 10 (2) kb downstream of the annotated transcription start sites for RefSeq genes with annotated 5' UTRs.

Since overlaps in the sequence flanking adjacent genes could create artifactual results, we eliminated any overlaps so that our analysis considers only non-overlapping sequences. We sorted the genes into those with high versus low CpG content in their flanking sequence, after inspecting the bimodal distribution generated by the scoring function over all of the RefSeq promoters, as defined by Mikkelsen, T. S. et al. (Genome-wide maps of chromatin state in pluripotent and lineage-committed cells. *Nature* 448, 553-60, 2007). We then eliminated any gene sets that had fewer than 8 genes.

Chromatin Immunoprecipitation-pPCR Primer Pairs

DNA extraction was performed using Qiagen Purification Kit. Real-time PCR analysis was performed for STAT3, MYC, MAX and RXRA binding sites in microRNA promoters using the following primers:

STAT3		**Forward**	**Reverse**
miR-21	site 1	TGGAGTTTCTGTGCAAACTGTC	TGTGCGTCATCCTTATCCAA
	sites 2,3	TGACACAAGCATAAGTCATTTCC	TCCTCAGAGTAAGGTCAGCTCAG
miR-181b	site 1	CAGAAATCAAACCAAAATCTGTT	TGAGTGAAACTCAGTCAAGCTC
	site 2	CACATCCTCACTCCACCCTA	AGTCCCAGCAGAAGTGAAGG
	site 3	CTGATTTCTCTACTGGCCCTTC	GCCACGTGCTCCTTTCTTAT
miR-210	site 1	CACACCAGGCTGCTGCAC	AGCAGTGGCCGCACTTAG
miR-132	site 1	CACGTGGGATCTTGACTCG	ACCGTGGCTTTCGATTGTTA
	site 2	AGCGGGGAATTTAGGAAATG	CCGGAAAGTTAACCCCTTGT
MYC			
miR-148a	site 1	TCGTGTCAAGTCAGCAGGTT	AGAGGCTGGTGGGCAGAAG
let-7a3	site 1	GGGCAGAAAATGAGATCCAG	GACCCTAACAGCCCAGCAC
miR-335	site 1	GTGAAGGCCGAGAACCTCT	CCCGCCTCTTACCTGATTC
MAX			
miR-148a	site 1	TCGTGTCAAGTCAGCAGGTT	AGAGGCTGGTGGGCAGAAG
miR-132	site 1	GTCCCTTTCGGACTCAGGAC	CTCCCCTTCCCTTCCCTTC
miR-181b	site 1	TGATTTCATTCGCTGGAATTT	AACATCAAGACTGCAGTTCAGC
miR-210	site 1	CATGGAGCTGAAGGTGTGG	CCTATTGCTTGGGCTAGTGC
miR-148b	site 1	AGCGCCAGTGTTAAAGGCTA	TCCATGGGGAACAGAAGAAG
miR-335	site 1	GGGTGCCCATACGAGGTG	GCGAGGGTTGTGTGACTTTT
RXRA			
miR-148a	site 1	CTTGACTTTTGCCGACGTG	GAGGGAACCTGCTGACTTGA
miR-132	site 1	GTCCCTTTCGGACTCAGGAC	CTCCCCTTCCCTTCCCTTC
miR-181b	site 1	CGGTAAAATATCCCAAATGTTTC	TTGTTGACACTCTATGAAGGAAAA
miR-210	site 1	AGAGCGAGCCTTGCAGGT	AGGGAGCACTTTCCCTGGT
miR-148b	site 1	TCAAAGCATATTCTTCTGTCCTT	TGTAAAGTACCTAAAAGAAGGGAACTT
miR-335	site 1	GGGTGTGACCGAGTGGTAGA	CCTCACCTCACACCTTCTTCA

Figure S1

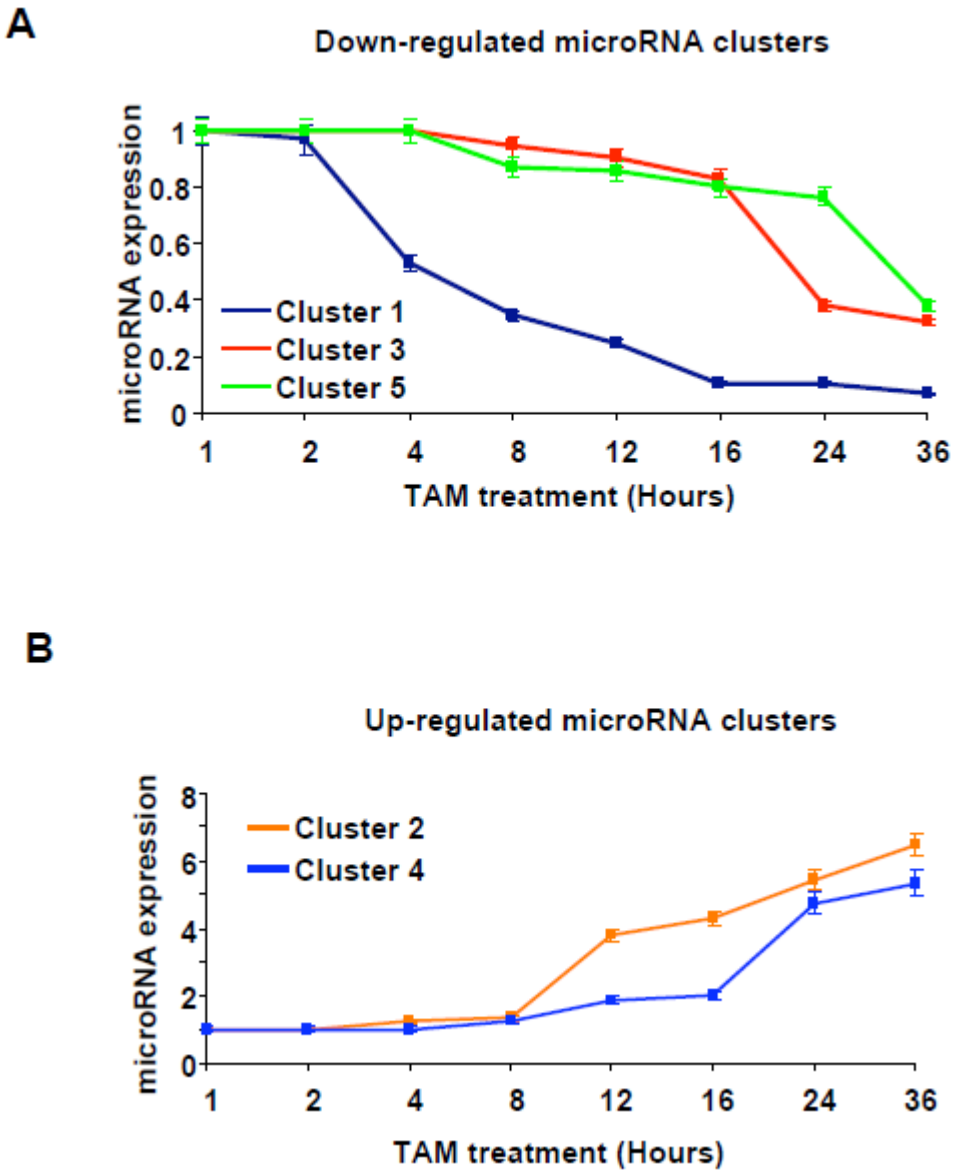

Figure S1, related to Figure 1. MicroRNA Clusters during ER-Src Transformation
(A) Three microRNA clusters were down-regulated during ER-Src transformation. Specifically, cluster 1 was down-regulated early (4 hr) during transformation while clusters 3 and 5 were down-regulated later (16-24 hr) during transformation.
(B) Two microRNA clusters were up-regulated during transformation. Both clusters are up-regulated 8-12 hr post TAM treatment. The data are presented as the average expression between different microRNAs in the same cluster.

Figure S2

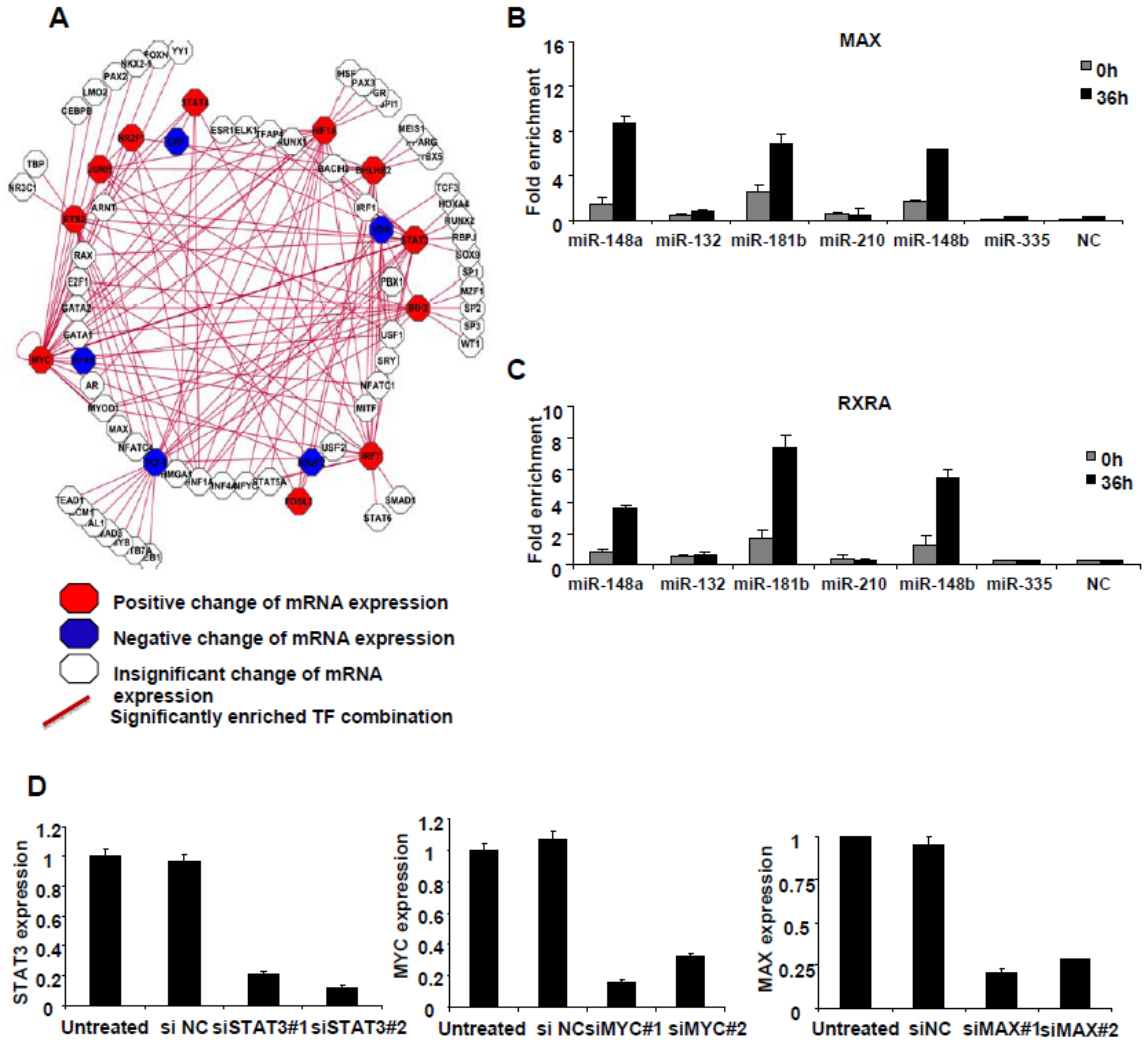

Figure S2, related to Figure 3. Transcription Factor Gene Networks

(A) Gene network including all significant transcription factor combinations in promoter areas for the 13 functional microRNAs (TF1 is connected with edge to TF2 if this combination is significantly enriched in the inspected promoter areas compared to background), according to Lever algorithm analysis, and for which at least one TF is differentially expressed.

(B and C) MAX (B) and RXRA (C) occupancy (fold enrichment) at the miR-148a, miR-132, miR-181b, miR-210, miR-193a, miR-148b and miR-335 loci as determined by ChIP of cross-linked cells that were or were not treated with TAM. The data are presented as mean ± SD of three independent experiments.

(D) Efficiency of STAT3, MYC, MAX and RXRA inhibition by different siRNAs. 100 nM of siSTAT3#2 inhibited more efficiently STAT3 expression in comparison to 100 nM of siSTAT3#1. Also 80 nM of siMYC#1 inhibited more efficiently MYC expression in comparison to 80 nM of siMYC#2. Thus, we decided to use for further experiments siSTAT3#2 and siMYC#1 to inhibit STAT3 and MYC expression levels, respectively.

Figure S3

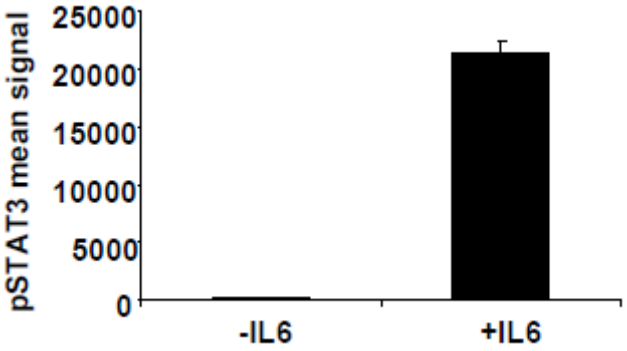

Figure S3, related to Figure 4. Assessment of pSTAT3 Nuclear Levels in MCF10A Cells

MCF10A cells were treated with IL6 (50 ng/ml) and 24 hr later pSTAT3 nuclear levels were assessed by ELISA assay. The data are presented as mean ±SD of three independent experiments.

Figure S4

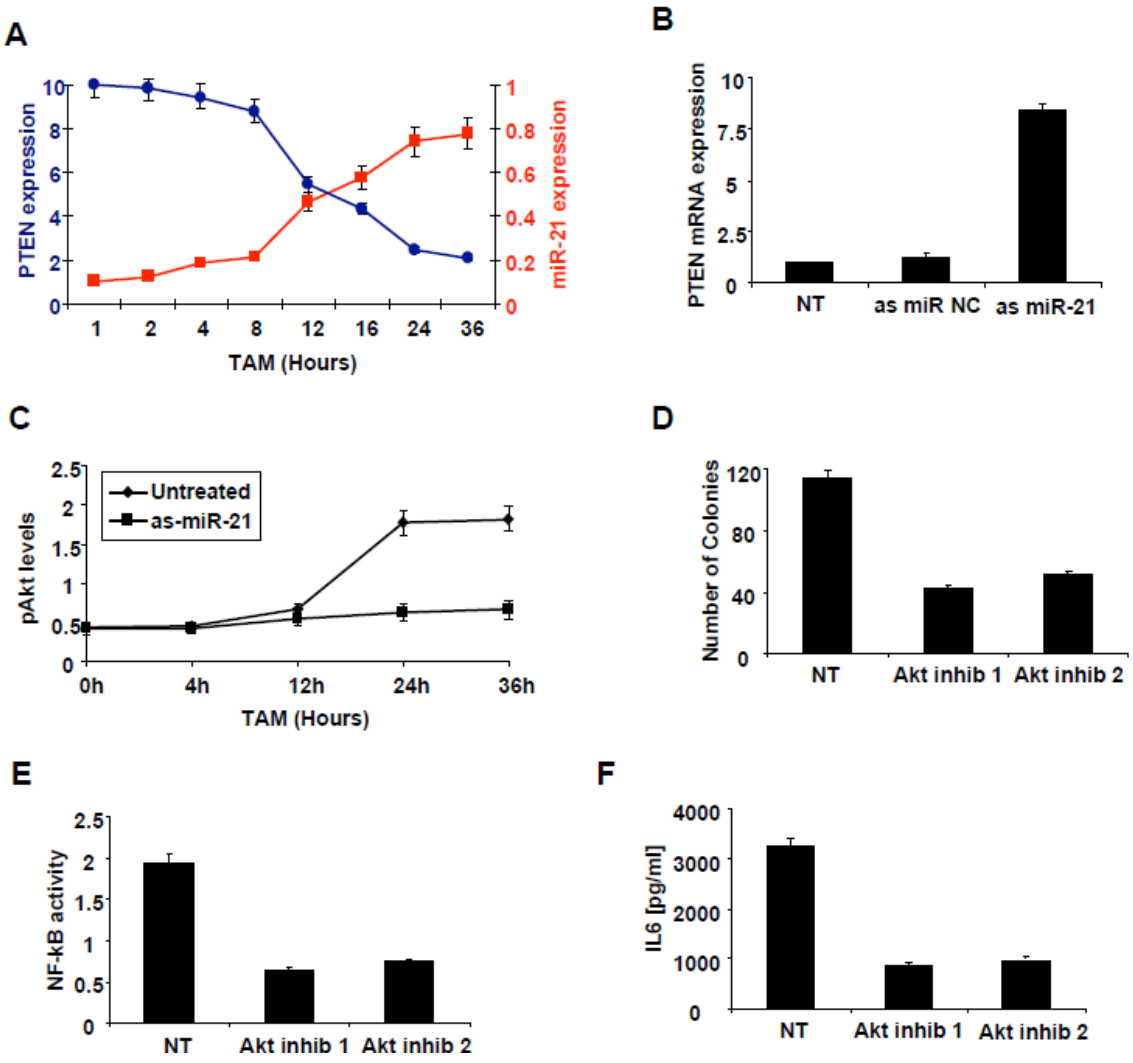

Figure S4, related to Figure 5. miR-21 Targets Directly PTEN Tumor Suppressor Gene Regulating Akt Pathway

(A) PTEN mRNA and miR-21 expression levels in different time points during ER-Src transformation.

(B) PTEN expression levels in ER-Src cells after treatment with antisense-miR-21 (as-miR-21) or antisense-miR-negative control (as-miR-NC). The data are presented as mean ±SD of three independent experiments.

(C) Akt phoshorylation levels (Ser473) assessed by ELISA assay in ER-Src cells treated with as-miR-21. The data are presented as mean ±SD of three independent experiments.

(D) Soft agar colony assay in transformed ER-Src cells treated with two different Akt inhibitors.

(E) NF-KB activity assessed by ELISA assay in ER-Src cells treated with two different Akt inhibitors.

(F) IL6 production (pg/ml) in ER-Src cells treated with two different Akt inhibitors.

Figure S5

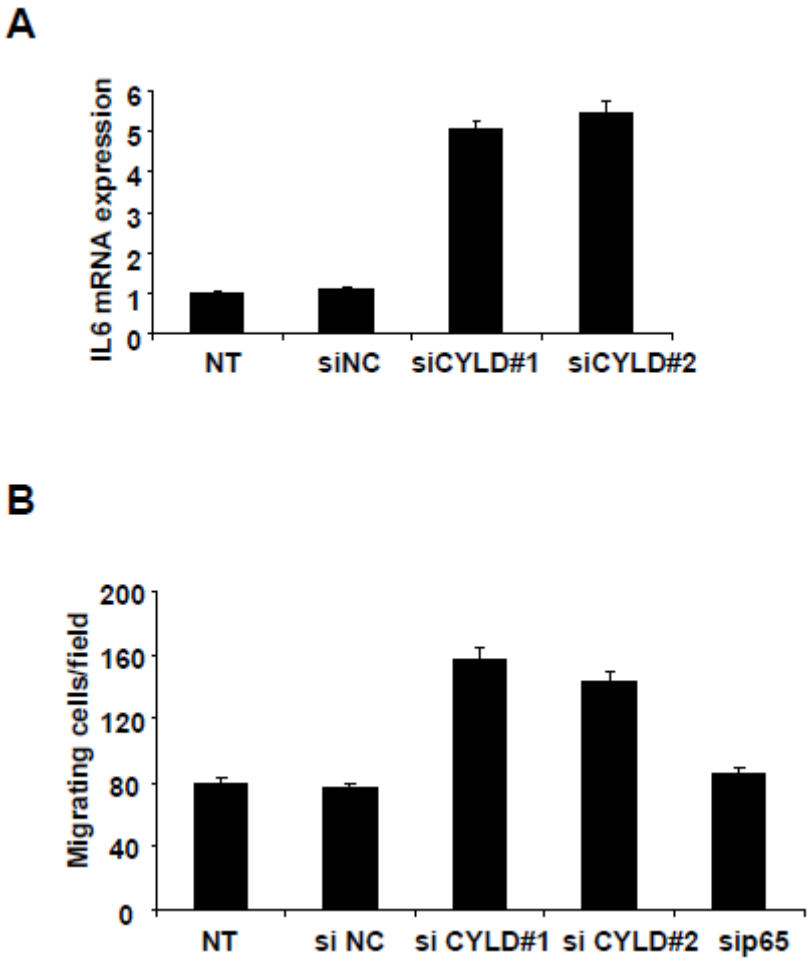

Figure S5, related to Figure 6. CYLD Suppression Induces MCF10A Cellular Transformation through NF-κB Pathway

(A and B) IL6 mRNA expression assessed by real-time PCR analysis (A) and migration assay in ER-Src cells treated with two different siRNAs against CYLD (B). The data are presented as mean ±SD of three independent experiments.